Time-dependent evolution process of Sb_2Te_3 from nanoplates to nanorods and their Raman scattering properties*

Xiu-Qing Meng(孟秀清)[1,†], Ning Tang (汤宁)[1], Mian-Zeng Zhong(钟绵增)[2], Hui-Qun Ye(叶慧群)[1], and Yun-Zhang Fang(方允樟)[1,‡]

[1] *Zhejiang Provincial Key Laboratory of Solid State Optoelectronic Devices, Zhejiang Normal University, Jinhua* 321004, *China*
[2] *State Key Laboratory of Superlattices and Microstructures, Institute of Semiconductors, Chinese Academy of Sciences, Beijing* 100083, *China*

(Received 14 March 2016; revised manuscript received 3 May 2016; published online 25 Augst 2016)

High-quality Sb_2Te_3 nanostructures are synthesized by a simple hydrothermal method. The morphologies of the nanostructures change from hexagonal nanoplates to nanorods with the extension of growth time. Secondary nucleation is the dominant factor responsible for the change of the morphologies. Structural analyses indicate that all the obtained nanostructures are well crystallized. IR-active phonons are mainly observed in the Raman spectra of the nanoplates and nanorods. The slight deviations are observed in the Raman modes between the nanoplates and nanorods, which could originate from confinement effect in the nanostructures.

Keywords: Sb_2Te_3 nanostructures, evolution process, confinement effect

PACS: 71.20.Nr, 74.25.Gz, 74.25.Kc **DOI:** 10.1088/1674-1056/25/10/107105

1. Introduction

Recently, great effort has been made to study nanostructured thermoelectric (TE) materials. The great improvement in the dimensionless figure of merit (ZT) has been achieved both theoretically and experimentally[1–4] due to both a high density of states and an increased phonon scattering or reduced lattice thermal conductivity in nanosystems.[1,5] Antimony telluride (Sb_2Te_3), a well-known narrow band-gap thermoelectric material with high ZT, has attracted considerable fundamental and technological interests for decades because of its potential applications in a stable ohmic back contact in high-efficiency solar cell devices,[6,7] mini power-generation systems and microcoolers, CCD technology, infrared detectors[8–12] and non-volatile phase change memory devices because of its ability to reversibly transform between amorphous to crystalline states.[13–16]

Although the controllable syntheses of TE nanostructures have been extensively studied by various methods,[17–24] the evolution process from nanoplates to nanorods with time has not been reported. Here in this work, we synthesize Sb_2Te_3 nanoplates by a simple hydrothermal method and for the first time observe the evolution process of the nanostructures from nanoplates to nanorods with reaction time.

2. Experimental details

The synthesis of Sb_2Te_3 nanostructures was carried out by the hydrothermal method. Typically, 0.114-g (0.5 mmol) $SbCl_3$ was dissolved in 3-ml deionized water, with 0.2-g tartaric acid simultaneously dissolved in another 3-ml deionized water under vigorous stirring. The two parts of the solutions were then mixed under continuous stirring. During this step, 0.178-g K_2TeO_3 (0.7 mmol) was dissolved in 20-ml $NH_3{\cdot}H_2O$, followed by dipping 8 ml of $NH_2{\cdot}H_2O$, thus forming a uniform transport solution. Then the uniform transport solution was added to the $SbCl_3$ solution under further stirring. The mixture was transferred to a teflon-lined stainless steel autoclave and sealed. The autoclave was placed in a pre-heated oven at 180 °C for various times, varying between 5 h and 48 h, and then naturally cooled to room temperature. The black precipitate obtained was filtered, washed with distilled water and ethanol several times until the filtrate became colorless, and then dried in a vacuum at 80 °C for 10 h in sequence. The structural characterizations of the samples were performed with x-ray diffraction (XRD) technique with using Cu Ka irradiation and field emission scanning electron microscopy (FESEM) images on a Hitachi S-4800 microscope instrument at an accelerating voltage of 10 kV. Raman spectrum was measured using a micro-Raman spectrometer with 514-nm laser as an excitation source.

3. Results and discussion

Figure 1 shows the x-ray powder diffraction data of the prepared powders obtained at pre-heating temperature of 80 °C for 5, 24, and 48 h, respectively. Evidently, all the peaks

*Project supported by the National Natural Science Foundation of China (Grant Nos. 11104250 and 61274099), the Fund from the Science Technology Department of Zhejiang Province, China (Grant No. 2012C21007), and the Fund for the Zhejiang Provincial Innovation Team, China (Grant No. 2011R50012).

†Corresponding author. E-mail: xqmeng@semi.ac.cn
‡Corresponding author. E-mail: fyz@zjnu.cn

© 2016 Chinese Physical Society and IOP Publishing Ltd

in the patterns of the samples can be indexed according to the power diffraction card of Sb_2Te_3 (JCPDS: 71-0393).

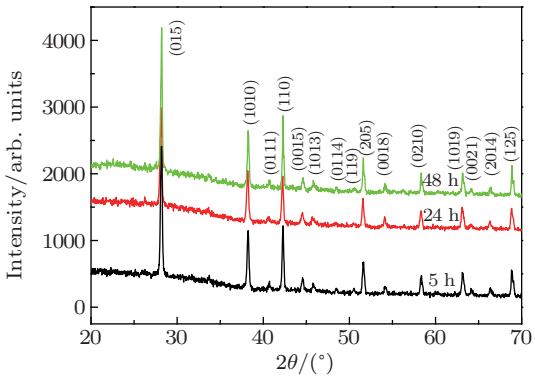


Fig. 1. (color online) XRD patterns of the nanostructures obtained at pre-heating temperature 80 ° C for 5, 24, and 48 h, respectively, indicating the samples have similar crystal quality.

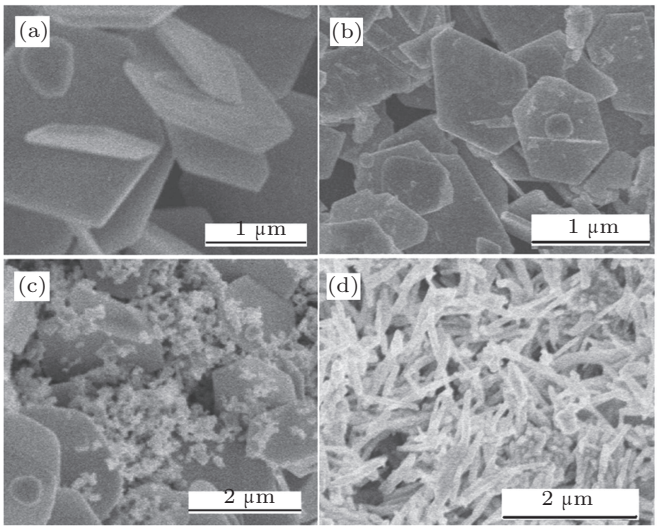


Fig. 2. SEM images of the nanostructures obtained for growing times of 5 h (a), 24 h (b), 36 h (c), and 48 h (d), which indicate the evolution process of the nanostructures from hexagonal nanoplates to nanorods.

No obvious diversity is observed among these samples.

However, the morphologies change greatly with the increase of reaction time as shown in Figs. 2(a)–2(d). From the evolution processes of the four samples we can find that at the beginning of the reaction (5 h) regularly shaped hexagonal nanoplates are formed with diameters of 1 μm–1.5 μm and thickness of 100 nm–120 nm as shown in Fig. 2(a), with prolonging reaction times to 24 h, small nanodots combined with short nanorods gradually appear on the surface of the nanoplates and in the gap between two nanoplates, and the sizes of the nanodots are in a range of about 100 nm–150 nm. When the reaction time reaches up to 36 h, more dots and small rods appear, the nanodots have a tendency to grow into nanorods. With further extending the reaction time up to 48 h, the samples are almost composed of nanorods in the whole observed region, no nanoplates are detected at this stage, implying that the samples are totally converted to nanorods. We speculate the evolution mechanism of the nanostructures in morphologies with time should be as follows. Hexagonal nanoplates of Sb_2Te_3 are easy to obtain as reported by most of the research.[25–27] In the original growth stage (5 h in our case), the precursors crystallize into hexagonal nanoplates, with expanding the growth time, secondary nucleation occurs on the surfaces of the nanoplates (24 h in our case), as a result, small nanodots are observed on the surfaces of nanoplates: the nanoplates act as nucleation sites. Further prolonging the growth time, the nanodots grow into short rods, and finally nanorods dominate when the growth time increases up to 48 h. The schematic growth diagram is shown in Fig. 3.

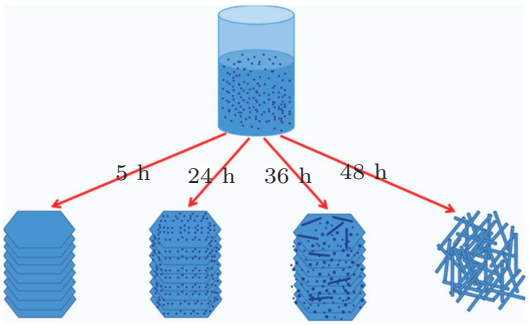


Fig. 3. (color online) Schematic diagram of evolution process of Sb_2Te_3 nanostructures from hexagonal nanoplates to nanorods.

Previous studies showed that Raman spectroscopy is a powerful tool for identifying the structures of the crystals. The extensive Raman studies are conducted on these nanostructures. Like other V_2VI_3 compounds, Sb_2Te_3 crystallizes into a layer structure with the symmetry $R\bar{3}m$ (D^5_{3d}). It shows therefore strong anisotropic behavior. There are five atoms per unit cell and consequently Sb_2Te_3 exhibits 15 phonon modes for each wave vector K.[28,29] In our sample we mainly observe IR-active phonons. Figures 4(a) and 4(b) present the representative Raman scattering spectra of the samples synthesized for 5 h and 48 h, in the case of 5-hour synthesized sample, six Raman modes located at 119, 142, 190, 252, 371, 451 cm^{-1} are observed, which correspond to the characteristic modes of E_u^{2a} (LO), $2A_{1g}$, $2E_u^{2a}$ (TO), $2E_u^{2a}$ (LO), $2E_u^{2a}$ (TO) +$2E_u^{2a}$ (LO), and $3E_u^{2a}$ (LO) of Sb_2Te_3, while the Raman modes of nanorods remain nearly the same as those of nanoplates, except 2 cm^{-1} of blue shift for each of the 119, 371, and 452 cm^{-1} Raman modes. Two reasons may be responsible for the change of the Raman modes: one is due to the breaking of symmetry in nanocrystals, which leads to the conversion of the original prohibited transmission into allowed transmission, correspondingly some new peaks emerge compared with the scenario for its bulk material. The other reason is that the confinement is anisotropic in the nanostructure, which causes the shifts of Raman modes, for it has a different effect on a different mode, as a result some modes shift while the others keep unchanged.[30]

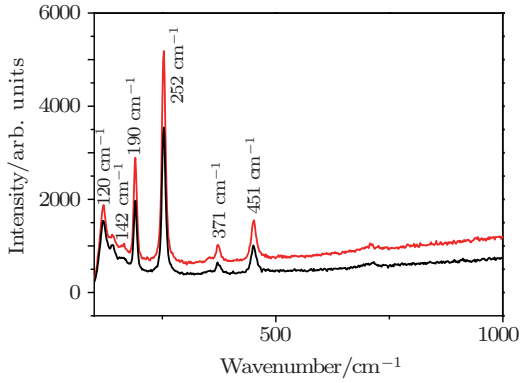


Fig. 4. (color online) Raman spectra of the as-synthesized nanoplates (black curve) and nanorods (red curve).

4. Conclusions

In this work, we successfully synthesize Sb_2Te_3 nanostructures and observe the evolution process from nanoplates to nanorods with growth time extending from 5 h to 48 h. A brief growth mechanism is presented to illustrate the evolution process. In addition, all the obtained nanocrystals are well crystallized. The Raman spectra of the nanostructures indicate that the samples are highly crystallized. The small deviation is observed between the nanoplates and nanorods, and caused by anisotropic confinement.

References

[1] Hicks L D and Dresselhaus M S 1993 *Phys. Rev. B* **47** 12727
[2] Hicks L D and Dresselhaus M S 1993 *Phys. Rev. B* **47** 16631
[3] Harman T C, Taylor P J, Spears D L and Walsh M P 2000 *J. Electron. Mater.* **29** L1
[4] Hicks L D, Sun T C, Harman X and Dresselhaus M S 1996 *Phys. Rev. B* **53** R1049
[5] Venkatasubramaniam R, Siivola E, Colpitts T and Quinn B O 2001 *Nature* **413** 597
[6] Romeo N, Bosio A, Tedeschi R, Romeo A and Canevari V 1999 *Sol. Energy Mater. Sol. Cells* **58** 209
[7] Abken A E and Bartelt O J 2002 *Thin Solid Films* **403–404** 216
[8] Shi W D, Yu J B, Wang H S and Zhang H J 2006 *J. Am. Chem. Soc.* **128** 16490
[9] Christian P and O'Brien P 2005 *J. Mater. Chem.* **15** 4949
[10] Zou H, Rowe D M and Min J J 2001 *Vac. Sci. Technol. A* **19** 899
[11] ElMandouh Z S 1995 *J. Mater. Sci.* **30** 1273
[12] Das V D, Soundararajan N and Pattabi M 1987 *J. Mater. Sci.* **22** 3522
[13] Wuttig M and Yamada N 2007 *Nat. Mater.* **6** 824
[14] Lankhorst M H R, Ketelaars B W S M M and Wolters R A M 2005 *Nat. Mater.* **4** 347
[15] Lee S H, Jung Y and Agarwal R 2007 *Nat. Nanotechnol.* **2** 626
[16] Jung H S and Myung N V 2011 *Electrochimica Acta* **56** 5611
[17] Prieto A L, Sander M S, Martin M S, Gronsky R, Sands T and Stacy A M 2001 *J. Am. Chem. Soc.* **123** 7160
[18] Jin C G, Xiang X Q, Jia C, Liu W F, Cai W L, Yao L Z and Li X G 2004 *J. Phys. Chem. B* **108** 1844
[19] Toprak M, Zhang Y and Muhammed M 2003 *Mater. Lett.* **57** 3976
[20] Yu S H, Yang J, Wu Y S, Han Z H, Lu J, Xie Y and Qian Y T 1998 *J. Mater. Chem.* **8** 1949
[21] Wang W Z, Poudel B, Wang D Z and Ren Z F 2005 *Acta Mater.* **17** 2110
[22] Wang W Z, Poudel B, Yang J, Wang D Z and Ren Z F 2005 *J. Am. Ceram. Soc.* **127** 13792
[23] Zhang HT, Luo X G, Wang C H, Xiong Y M, Li S Y and Chen X H 2004 *J. Cryst. Growth* **265** 558
[24] Shi W, Zhou L, Song S, Yang J and Zhang H 2008 *Adv. Mater.* **20** 1892
[25] Zhou N, Chen G, Zhang X S, Xu Y C, Xu B R and Li M Q 2014 *RSC Adv.* **4** 2427
[26] Liang L X, Deng Y, Wang Y and Gao H L 2013 *J. Nanopaticles Res.* **16** 2138
[27] Hao G, Qi L X, Fan Y P, Xue L, Peng X Y, Wei X L and Zhong J X 2013 *Appl. Phys. Lett.* **102** 013105
[28] Richter W, Krost A, Nowak U and Anastassakis E 1982 *Physica B-Condens. Matter* **49** 191
[29] Kim Y, Chen X, Wang Z, Shi J, Miotkowski I, Chen Y P, Sharma P A, Sharma A L L, Hekmaty M A, Jiang Z and Smirnov D 2012 *Appl. Phys. Lett.* **100** 071907
[30] Meng X Q, Shen D Z, Zhang J Y, Zhao D X, Lu Y M, Dong L, Zhang Z Z, Liu Y C and Fan X W 2005 *Solid State Commun.* **135** 179